Reaction Chemistry & Engineering

ROYAL SOCIETY OF CHEMISTRY

PAPER

View Article Online
View Journal | View Issue

Cite this: *React. Chem. Eng.*, 2020, 5, 1783

Hydrogenolysis of alginic acid over mono and bimetallic ruthenium/nickel supported on activated carbon catalysts with basic promoters

Seungdo Yang, Hyungjoo Kim and Do Heui Kim *

Received 31st May 2020,
Accepted 20th July 2020

DOI: 10.1039/d0re00224k

rsc.li/reaction-engineering

Hydrogenolysis of alginic acid, derived from macroalgae, over Ru, Ni and Ru–Ni supported on activated carbon catalysts was performed in a batch reactor using NaOH, $CaCO_3$, $Ca(OH)_2$, and $Mg(OH)_2$ as basic promoters. Among the promoters used, NaOH provides the highest carbon efficiency and yield of glycols, such as ethylene glycol and 1,2-propanediol. In addition, various organic acids such as lactic acid, glycolic acid, and formic acid were produced in the form of salts. The hydrogenolysis of potential intermediates such as sorbitol, mannitol, lactic acid, and glycolic acid demonstrated direct conversion of alginic acid to glycols without sugar alcohols or organic acids as reaction intermediates. Furthermore, Ru–Ni bimetallic catalysts as a function of the Ni/Ru molar ratio were used to increase the yield of and selectivity to glycols. The highest yield of glycols, 24.1%, was obtained when the Ni/Ru molar ratio was 1 : 1, due to the enhanced interaction between Ru and Ni based on H_2-TPR.

1. Introduction

Biorefinery, in which renewable resources are utilized on a large scale, is a potential alternative based on biomass feedstocks.[1–3] Algal biomass, also known as the third-generation biomass, is inedible, lignin-free, and shows rapid growth, and has significant advantages in biorefinery.[4,5] As the main component of macroalgae, alginic acid is a good carbon source for the production of various value-added chemicals such as acids and alcohols. Alginic acid is a polyuronide consisting of two types of hexuronic acid, D-mannuronic acid (M) and L-guluronic acid (G), connected by β-1,4-glycosidic bonds. The two units combine randomly to create polymer rings carrying carboxyl (–COOH), ether (–COC–), and hydroxyl (–OH) functional groups, which enable the prediction of reaction pathways and the design of platform chemicals converted from alginic acid. Based on such prediction, the hydrothermal decomposition of alginic acid was conducted under various conditions. Our group investigated the formation of sugar alcohols such as sorbitol and mannitol *via* hydrogenation of alginic acid.[6–8] However, the hydrogenolysis of alginic acid to glycols such as ethylene glycol (EG) and 1,2-propanediol (PDO), which are shorter chain polyols than sugar alcohols, has yet to be reported. The glycol products can be used as surfactants, antifreeze compounds, and monomers in the synthesis of polyester fibers, and as chemicals in the pharmaceutical industry.[9,10] Therefore, it is expected that the efficient conversion of alginic acid into glycols provides a platform to further improve the utilization of alginic acid as a biomass feedstock.

Meanwhile, the reaction mechanisms underlying the hydrogenolysis of biomass-derived feedstocks including cellulose, sugar alcohols and glycerol into glycols have been investigated.[11–21] Since the hydrogenolysis reaction occurs *via* multiple steps, it is difficult to determine the precise reaction pathway under various reaction conditions. Nonetheless, several mechanisms of hydrogenolysis have been proposed based on experimental results. Montassier *et al.*[18] suggested that sugar alcohol forms an intermediate with unsaturated bonds *via* dehydrogenation and undergoes a C–C bond cleavage *via* a retro-aldol reaction or a C–O bond cleavage by dehydration under basic conditions. In addition, other mechanisms have been proposed, including decarbonylation to explain the terminal C–C cleavage and the retro-Claisen reaction and the retro-Michael reaction based on by-product analysis.[18] The authors reported that both a basic promoter and a metal catalyst play a role in the hydrogenolysis.

Based on these reaction pathways, several research groups performed hydrogenolysis using metal catalysts along with basic promoters.[9,22–26] Ru-Based catalysts have been the most frequently used. For instance, Mariscal *et al.*[9] reported that the yield of glycols (the sum of EG and PDO) from sorbitol increased significantly over Ru supported on alumina with $Ca(OH)_2$ as a base additive. While the dehydrogenation/hydrogenation reactions were activated by the Ru catalyst, the C–C bond cleavage *via* a retro-aldol reaction was promoted by

School of Chemical and Biological Engineering, Institute of Chemical Processes, Seoul National University, Seoul, 08826, Republic of Korea.
E-mail: dohkim@snu.ac.kr

a basic promoter, especially $Ca(OH)_2$, as well as a basic support, resulting in improved carbon efficiency and selectivity to glycols. Also, Besson *et al.*[25] reported that the addition of a basic promoter shifted the hydrogenolysis reaction pathway of xylitol from fast epimerization and decarbonylation to retro-aldol reaction over Ru-based catalysts. Thus, basic promoters play a crucial role in changing the selectivity to glycols.

Ni generally enhances the activity in the hydrogenation and hydrogenolysis of biomass feedstock.[9,13,27–31] According to Banu *et al.*,[27] among Ni, Pt, and Ru supported on NaY catalysts, Ni–NaY was the most efficient catalyst in the hydrogenolysis of sorbitol to EG and PDO with a selectivity of 7% and 69%, respectively. Ni has also been used as a bimetallic catalyst in combination with other noble metals. Pereira *et al.*[32] reported that Ru–Ni bimetallic catalysts supported on activated carbon showed superior activity in the hydrolytic hydrogenation of cellulose to sorbitol. The authors suggested that the close interaction between Ru and Ni facilitates the conversion of cellulose and the selectivity to sorbitol. Hence, it would be interesting to utilize the bimetallic Ru–Ni supported on activated carbon in the hydrogenolysis of alginic acid.

The main objective of this study is to establish the optimum reaction system for the conversion of alginic acid to glycols such as EG and PDO over Ru-based activated carbon catalysts in a basic solution. To begin with, the characteristics of the prepared catalysts were investigated *via* X-ray diffraction (XRD), N_2 adsorption–desorption, and H_2-temperature-programmed reduction (H_2-TPR). We optimized the reaction parameters such as reaction time, temperature, hydrogen pressure, and base concentration in the hydrogenolysis reaction. Subsequently, various basic promoters such as $CaCO_3$, $Ca(OH)_2$, $Mg(OH)_2$, and NaOH were introduced in the hydrogenolysis over Ru-based activated carbon catalysts under the optimized reaction conditions. Finally, Ni, which enhances the activity in the hydrogenolysis, was utilized in bimetallic Ru–Ni catalysts to determine the optimum Ni/Ru molar ratio.

2. Experimental procedure

2.1 Materials and chemicals

Activated carbon as the support and alginic acid from brown algae as the reactant were purchased from Sigma-Aldrich. The metal precursors $RuCl_3{\cdot}xH_2O$ (ruthenium chloride hydrate) and $Ni(NO_3)_2{\cdot}6H_2O$ (nickel nitrate hexahydrate) were purchased from Alfa-Aesar. Hexitols (HOL: sorbitol, mannitol, and galactitol), pentitols (POL: xylitol, arabitol, and adonitol), tetritols (TOL: erythritol and threitol), EG, and PDO were obtained from Alfa-Aesar, and were utilized as analytical standards or reactants except for threitol (from TCI, Tokyo Chemical Industry). Organic acids (lactic acid, glycolic acid, and formic acid) and basic promoters ($CaCO_3$, $Ca(OH)_2$, $Mg(OH)_2$, and NaOH) were purchased from Sigma-Aldrich. For derivatization of liquid-product samples, *N*,*O*-bis(trimethylsilyl)trifluoroacetamide (BSTFA) was obtained from Alfa-Aesar. All chemicals were utilized without further purification or treatment.

2.2 Catalyst preparation

A wet impregnation method was used for the preparation of Ru-based activated carbon catalysts. The loading amount of the metals such as Ru and Ni in monometallic activated carbons, which are denoted as Ru/AC and Ni/AC, respectively, was 5 wt%. Ru-Based bimetallic catalysts were prepared as a function of the Ni/Ru molar ratio, and at this time, the loading amount of Ru was maintained at 5 wt%. The resultant bimetallic catalysts were denoted as $RuNi_x$/AC, where x stands for the molar ratio of Ni to Ru. A 150 mL solution containing metal precursors was stirred with 2 g of activated carbon for 2 h, and then evaporated using a rotary evaporator followed by drying in an oven at 105 °C overnight. The dried powders were reduced in a muffle furnace at 250 °C (Ru/AC) and 500 °C (Ni/AC and $RuNi_x$/AC) for 2 h under 5% H_2/N_2 stream (100 ccm), and the reduced catalysts were passivated under 3% O_2/N_2 (100 ccm) at room temperature.

2.3 Catalyst characterization

Inductively coupled plasma-atomic emission spectroscopy (ICP-AES) was used (SHIMADZU/ICPE-9000) to determine the content of Ru and Ni in the catalysts. The N_2 adsorption–desorption isotherms were obtained using a BELSORP-mini II (BEL Japan Inc.). The catalysts were pretreated in a vacuum at 200 °C for at least 4 h before N_2 physisorption analysis. The results of the analysis were utilized to calculate the surface area of the catalysts *via* the Brunauer–Emmett–Teller (BET) method. XRD patterns were obtained with a powder X-ray diffractometer (Smartlab, Rigaku) operated at a current of 30 mA and a voltage of 40 kV. H_2-TPR profiles were obtained using a BELCAT-II catalyst analyzer (BEL Japan Inc.). The pretreated samples were heated to 900 °C (10 °C min^{-1}) in 5% H_2/Ar flow.

2.4 Catalytic activity

The hydrogenolysis of alginic acid was carried out in a 100 mL autoclave (Parr Instrument Company) after charging alginic acid or other reactants (0.3 g), deionized water including basic promoters (30 mL), and a catalyst (0.1 g).The autoclave was heated to the target temperature (8–9 °C min^{-1}) while stirring at 1000 rpm under high-pressure H_2 gas after purging three times with 99.999% Ar to remove the air inside. The hydrogenolysis reaction was conducted at 150–240 °C for 0.3–4 h under 10–70 bar. After the reaction, the reactor was rapidly quenched in an ice-cold bath and the liquid-product in the reactor was collected manually.

2.5 Product analysis

C_2–C_6 polyols contained in the liquid-product were quantified *via* gas chromatography (GC, Agilent 6890 equipped with a

DB-5 column). For the derivatization of the liquid-sample, it was pretreated *via* silylation with BSTFA as reported by Lin *et al.*[33] High-performance liquid chromatography (HPLC using a VW detector, Agilent 1200 Series equipped with an Aminex HPX-87H column) at a column temperature of 65 °C and a flow rate of 0.6 mL min^{-1} in the presence of 5 mM sulfuric acid was used to quantify organic acids in the liquid-product. All of the polyols and organic acids were calibrated using the external standard. By-products such as char and gas-phase products, which are not included in the liquid-products, were measured based on the difference between the total organic carbon (TOC, Sievers 5310C (GE)) of the liquid-product and the standard TOC of alginic acid as reported in our previous study.[6] Based on the data obtained, the carbon yield was calculated as follows: $Y_{product}$ (%) = 100 × (number of carbon species in an organic compound/6) × (moles of an organic compound in the product mixture/moles of a repeating unit in alginic acid of 0.3 g). In addition, since the conversion of alginic acid, a polymer, cannot be calculated, carbon efficiency (E_c) was used to represent the conversion efficiency of the reaction system. E_c was calculated as follows: E_c (%) = Y_{HOL} + Y_{POL} + Y_{TOL} + Y_{BDO} + Y_{PDO} + Y_{EG} + Y_{LA} + Y_{GA} + Y_{FA} (HOL: sorbitol, mannitol, and galactitol; POL: xylitol, arabitol, and adonitol; TOL: erythritol and threitol; BDO: 1,2-butanediol; PDO: 1,2-propanediol; EG: ethylene glycol; LA: lactic acid; GA: glycolic acid; FA: formic acid).

3. Results and discussion

The surface area and atomic loading of the prepared catalysts are summarized in Table 1. All the metals supported on AC samples demonstrated a decrease in the BET surface area compared with the AC support, although no significant change was found in the BET surface area of the metal-containing samples as a function of the Ru/Ni molar ratio. The atomic loading of the metals in the catalyst matched strongly with the one initially designed, resulting in a reliable Ni/Ru ratio with about 10% error.

The crystallinity of Ru and/or Ni supported on activated carbon catalysts was analyzed by XRD. As shown in Fig. 1, no X-ray diffraction peaks assigned to Ru species were detected in any sample. It is suggested that amorphous RuO_2 formed or Ru with a small crystallite size was highly dispersed during the passivation process.[34] However, diffraction peaks were detected at 2θ = 44.5° and 51.9° attributed to metallic Ni in the Ni/AC sample. In the case of bimetallic Ru–Ni catalysts, as the amount of Ni added increased, the peak of metallic Ni turned sharper without shifting the peak position, indicating the crystallization of Ni rather than the formation of Ru–Ni alloy.

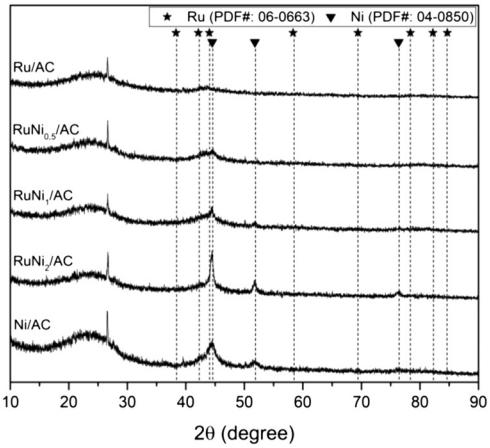

Fig. 1 XRD diffractograms of mono and bimetallic Ru–Ni supported on AC.

H_2-TPR was performed to elucidate the reductive property of metallic species in catalysts. As shown in Fig. 2, Ni/AC exhibited two broad reduction peaks at *ca.* 150–350 °C resulting from various interactions between nickel oxide phases and surface functional groups of activated carbon.[35] However, Ru/AC exhibited a reduction peak due to the reduction of RuO_x to Ru at *ca.* 130 °C.[7,34] All of the Ru–Ni bimetallic catalysts present a single peak of reduction suggesting the onset of a close interaction between Ni and Ru.[36,37] Notably, the reduction peak of Ru–Ni species shifted to a higher temperature by *ca.* 30 °C over $RuNi_1$/AC. It can be

Table 1 Surface area and atomic loading of mono and bimetallic Ru–Ni supported on AC

Catalyst	Surface area[a] (m^2 g^{-1})	Atomic loading[b] (wt%)		
		Ru	Ni	Ni/Ru[c]
AC	1032.5	—	—	—
Ru/AC	774.27	4.41	—	—
$RuNi_{0.5}$/AC	882.35	4.55	1.14	0.43
$RuNi_1$/AC	849.52	4.48	2.95	1.13
$RuNi_2$/AC	815.09	5.22	6.38	2.10
Ni/AC	845.21	—	5.85	—

[a] Calculated by the BET method. [b] Measured by ICP-AES. [c] Ni/Ru molar ratio.

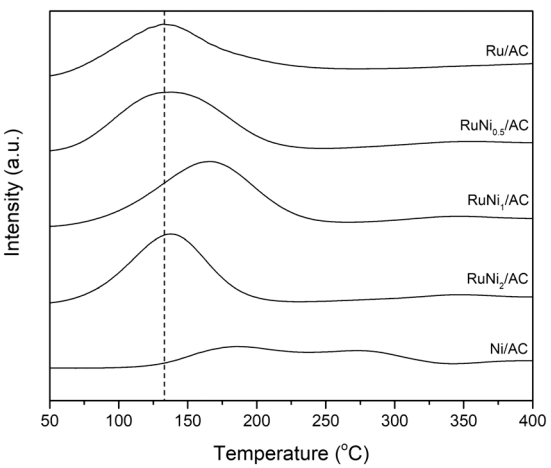

Fig. 2 H_2-TPR profiles of Ru and/or Ni supported on AC.

inferred that the interaction between Ru and Ni is the most intimate in the $RuNi_1$/AC sample among the samples. However, the reduction peak of $RuNi_2$/AC shifted to a low temperature again, suggesting that the interaction between Ru and Ni was partially weakened at high Ni loading, which is also evidenced by the single X-ray diffraction peaks arising from Ni in $RuNi_2$/AC. Therefore, it is inferred that the molar ratio of Ru and Ni affects the interaction between Ru and Ni species over the catalysts.

Fig. 3 presents the changes in various products as a function of reaction parameters including reaction time, temperature, hydrogen pressure, and base concentration over the Ru/AC catalyst. As shown in Fig. 3(a), the production of glycols was detected even in a relatively short reaction time. Also, note that the changes in the amount or distribution of the product were insignificant as the reaction time increased. Such a result was in line with our previous study, which reported that alginic acid sodium salt instantaneously decomposed into organic acids at high pH.[38] In addition, the yield of glycols did not differ significantly depending on the reaction temperature, whereas organic acids, especially lactic acid (LA), which was not produced at 150 °C, were produced significantly at 210 °C as demonstrated in Fig. 3(b). Under the conditions at 210 °C, the improved carbon efficiency (E_c) yielding value-added products is an encouraging result.[38–40] However, at temperatures above 210 °C, unidentified by-products were produced more abundantly. Therefore, the optimum reaction temperature was determined to be 210 °C, at which the carbon efficiency (E_c) increased with a stable yield of glycols. Hydrogen pressure is also one of the important parameters that influence the conversion of alginic acid (Fig. 3(c)). LA was predominantly produced compared with other products at 10 bar H_2 pressure. An increased H_2 pressure led to a decrease in the yield of LA with a simultaneous increase in the yield of EG, PDO, and BDO. However, when the pressure was higher than 50 bar, the extent of product distribution decreased. Based on this result, the optimum hydrogen pressure was found to be 50 bar. As shown in Fig. 3(d), the product yield as a function of NaOH concentration has a large effect on the change in the products. Fewer amounts of glycols and organic acids were produced in the 50 mM solution of NaOH, which is similar to the concentration of alginic acid (52 mM). It can be assumed that the low yield of glycols and organic acids in 50 mM NaOH solution is because alginic acid is titrated with NaOH resulting in few free bases for hydrogenolysis. Increasing the NaOH concentration to 100 mM led to a significant increase in the yield of glycols, which means that free bases participated in the hydrogenolysis reaction for C–C cleavage. However, in the case of 200 mM solution of NaOH, the yield of glycols decreased whereas the yield of organic acids, especially LA, increased compared with 100 mM NaOH. Various organic acids from alginic acid may exist in the form of salts under basic conditions. Maris *et al.*[16] reported that

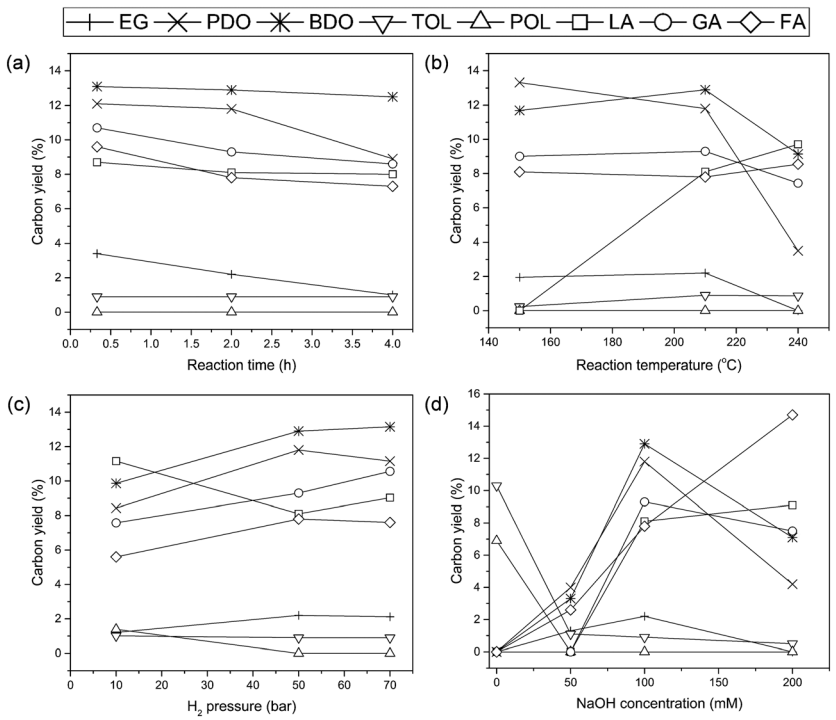

Fig. 3 Carbon yield during the hydrogenolysis of alginic acid as a function of the reaction parameters such as (a) reaction time (at 210 °C under 50 bar H_2 in 100 mM NaOH solution), (b) reaction temperature (for 2 h under 50 bar H_2 in 100 mM NaOH solution), (c) hydrogen pressure (at 210 °C for 2 h in 100 mM NaOH solution) and (d) NaOH concentration (at 210 °C for 2 h under 50 bar H_2). Product notation: EG = ethylene glycol, PDO = 1,2-propanediol, BDO = 1,2-butanediol, TOL = tetritols (erythritol and threitol), POL = pentitols (xylitol, arabitol, and adonitol), LA = lactic acid, GA = glycolic acid, FA = formic acid.

LA in the presence of a base can lead to the formation of lactate salt, resulting in the suppressed production of PDO during the hydrogenolysis of glycerol. In our results, it was found that the amount of LA produced was proportional to the NaOH concentration, suggesting that sodium lactate converted from free LA inhibited the production of glycols, especially PDO. However, the retro-aldol reaction related to the hydrogenolysis process is promoted by adsorbed hydroxyl groups under basic conditions.[16] Hence, the 100 mM NaOH solution, which yields the most glycols, is favorable in the hydrogenolysis although organic acid salts inhibit the production of glycols.

The hydrogenolysis of alginic acid was performed to investigate the role of the metal catalysts and the basic promoters under optimum reaction conditions. As summarized in Table 2, the presence or the absence of Ru/AC and the basic promoters caused a large change in product distribution. The total carbon yield, which is the sum of by-products calculated by TOC and E_c, does not add up to 100% due to unidentified liquid-products. The depolymerization of alginic acid under basic conditions proceeds to lead the formation of various products. For instance, methanol might be produced in the process of hydrogenolysis. M. Liu *et al.*[15] and P. Lazaridis *et al.*[14] suggested that methanol is produced *via* the C–C cleavage of polyols. However, methanol could not be quantified due to technical limitations in our HPLC analysis although it was confirmed that methanol was qualitatively produced. In addition to methanol, various polyols and organic acids may be formed. The addition of NaOH without Ru/AC resulted in the formation of LA and FA without producing glycols. This is in line with our previous study demonstrating the effect of pH on the conversion of alginic acid sodium salt resulting in the instantaneous formation of organic acids from alginic acid sodium salt at high pH.[38] However, when the reaction was conducted over Ru/AC without the basic promoters, no liquid-products containing fewer than three carbon species were detected resulting in the production of C_4 and C_5 sugar alcohols. Palkovits *et al.*[41] claimed that C–C cleavage occurs at the end of the carbon chain *via* decarbonylation rather than the retro-aldol reaction that leads to C_2/C_4 and C_3/C_3 fragments when Ru/AC is used in the hydrogenolysis of sorbitol under neutral or acidic conditions. Accordingly, it is suggested that C_4 and C_5 alcohols were formed *via* decarbonylation of C_6 sugar alcohols generated *via* hydrolytic hydrogenation of alginic acid under neutral conditions. Furthermore, it was also confirmed that the decomposition pathway under the conditions occurred *via* decarbonylation since no product of alcohols below C_4 was detected. Meanwhile, the addition of both metal catalysts and basic promoters led to produce various organic acids and shorter chain polyols such as glycols and BDO, whereas C_4–C_6 sugar alcohols were hardly produced. Likewise, the base promoters play an important role in reducing the amount of unnecessary by-products, which leads to improved carbon efficiency. As a result, it can be inferred that the decomposition of alginic acid proceeded *via* other pathways rather than the aforementioned decarbonylation reaction. Following the addition of other basic promoters, alginic acid was partially converted to short-chain polyols except for $Ca(OH)_2$, which lacked the activity for hydrogenolysis. However, $CaCO_3$ and $Mg(OH)_2$ were not appropriate as promoters due to their low carbon efficiencies of 42.4% and 25.5%, respectively. In other words, it is attributed to the larger production of unidentified products than the one with NaOH.

As shown in entries 1 and 3 in Table 2, the addition of the Ru catalyst to the NaOH solution altered the distribution and amount of the products by changing the hydrogenolysis pathway. Niemelä *et al.*[42,43] claimed that the decomposition of alginic acid to organic acids in the alkaline solution proceeds *via* direct degradation at the end of the chains or cleavage of internal glycosidic linkages. Our results demonstrate that the NaOH promoter has a large effect on both ends and insides of the chain, resulting in the production LA and FA. Furthermore, the basic promoter and catalyst showed a synergistic effect on the production of C_2 compounds such as GA and EG. In addition, the selectivity to LA and FA was reduced leading to the production of short-chain polyols. When Ru/AC was used with the NaOH promoter, the yield of by-products was 25.1%, which was approximately half the yield of by-products (49.7%) generated by Ru/AC in a neutral solution. Thus, the suppression of by-products is a significant synergistic effect of the Ru/AC catalyst in the presence of the NaOH promoter. Meanwhile,

Table 2 Product yields and carbon efficiency obtained during the hydrogenolysis of alginic acid over Ru/AC with various basic promoters[a]

Entry	Catalyst	Base	Liquid-product yield (%)								Other[b] (%)	E_c (%)
			EG	PDO	BDO	TOL	POL	LA	GA	FA		
1	None	NaOH	0	0	2.5	0.2	0.3	24.7	0	26.9	25.1	54.6
2	Ru/AC	None	0	0	0	10.3	6.9	0	0	0	49.7	19.4
3	Ru/AC	NaOH	2.2	11.8	12.9	0.9	0	8.1	9.3	7.8	25.1	53.0
4	Ru/AC	$Ca(OH)_2$	0	0	0	0	0	12.1	0	0	63.4	12.1
5	Ru/AC	$CaCO_3$	2.4	13.1	12.7	1.0	0.4	0	11.7	0	57.6	42.4
6	Ru/AC	$Mg(OH)_2$	2.1	11.0	3.6	0.5	0.3	6.7	0	0	37.7	25.5

[a] EG = ethylene glycol, PDO = 1,2-propanediol, BDO = 1,2-butanediol, TOL = tetritols (erythritol and threitol), POL = pentitols (xylitol, arabitol, and adonitol), LA = lactic acid, GA = glycolic acid, FA = formic acid; reaction conditions: at 210 °C for 2 h under 50 bar in 100 mM basic solution. [b] Calculated by TOC in the liquid-product.

the following assumptions can be made regarding the reaction pathway of the hydrogenolysis of alginic acid when the Ru/AC catalyst was used with the NaOH promoter. First, the polyols are produced *via* hydrogenolysis of C_6 sugar alcohols, such as sorbitol and mannitol, as intermediates. As shown in entries 1–3 in Table 3, sugar alcohols, which can be regarded as the intermediate step in the hydrogenolysis of alginic acid, were converted to shorter polyols and LA. In addition, the conversion of all the sugar alcohols was determined to be 100%. However, the EG-to-PDO ratio generated from the sugar alcohols was about 1 : 1 whereas the ratio derived from alginic acid was about 0.2 : 1 (Table 2, entry 3). Besides, BDO was rarely produced compared with the one from alginic acid, suggesting that it is not mediated *via* sugar alcohols obtained by the hydrolytic hydrogenation of alginic acid in the production pathway of glycols. Hence, the first assumption can be excluded. The second assumption is that the polyols are produced *via* hydrogenation of organic acids depolymerized from alginic acid. However, the organic acids were hardly reactive under severe hydrogenolysis reaction conditions, resulting in the reduced conversion of LA and GA (1.7% and 4.6%, respectively) as demonstrated in entries 4 and 5 in Table 3. Therefore, organic acids do not act as intermediates in the process of glycol production. Hence, we pay attention to the third assumption that glycols and organic acids are produced *via* separate reaction pathways. As demonstrated in entries 1–3 in Table 3, hydrogenolysis of sugar alcohols support the third assumption. Although the carbon number between HOL and POL differs, the changes in the selectivity to and yield of LA and FA were insignificant, suggesting that organic acids were obtained *via* a side effect in the hydrogenolysis of alginic acid in the basic solution. However, Ru/AC with the basic promoter is required for the selective hydrogenolysis to obtain glycols from alginic acid. Thus, it can be suggested that glycols and organic acids were produced *via* separate reaction pathways, which affect the hydrogenolysis of alginic acid into glycols and organic acids depending on the reaction parameters related to metals and basic promoters rather than the reaction time and temperature. Bimetallic Ru–Ni supported on activated carbon catalysts were prepared to further enhance the production of glycols. As shown in Fig. 4, Ru–Ni bimetallic catalysts show enhanced catalytic

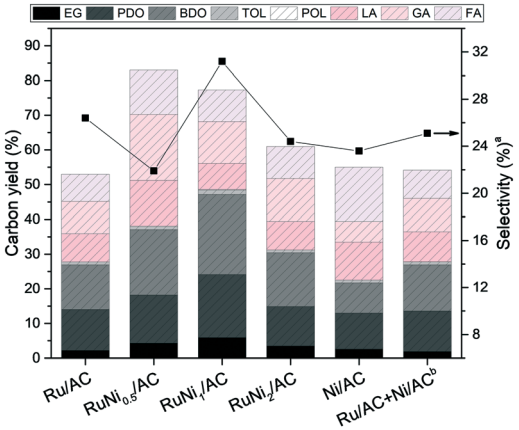

Fig. 4 Carbon yield and glycol selectivity during the hydrogenolysis of alginic acid over the catalysts as a function of the Ni/Ru molar ratio. Reaction conditions: at 210 °C for 2 h under 50 bar in 100 mM NaOH solution; product notation: EG = ethylene glycol, PDO = 1,2-propanediol, BDO = 1,2-butanediol, TOL = tetritols (erythritol and threitol), POL = pentitols (xylitol, arabitol, and adonitol), LA = lactic acid, GA = glycolic acid, FA = formic acid; [a] the selectivity to glycols = $(Y_{EG} + Y_{PDO})/(Y_{EG} + Y_{PDO} + Y_{BDO} + Y_{TOL} + Y_{POL} + Y_{LA} + Y_{GA} + Y_{FA}) \times 100$, [b] 8.8 wt% Ru/AC (50 mg) + 5.9 wt% Ni/AC (50 mg).

activity compared with Ru or Ni monometallic catalysts and physically mixed Ru and Ni catalysts. In the case of $RuNi_{0.5}$/AC, the glycol yield and the carbon efficiency (E_c) increased significantly from 14.0% to 18.2% and from 53.0% to 83.0%, respectively, compared with Ru/AC. It is reasonable to claim that the hydrogenolysis of alginic acid was more active in the presence of bimetallic catalysts. When the Ni/Ru molar ratio was 1 : 1, the yield of and selectivity to glycols and BDO were the highest even though the carbon efficiency (E_c) decreased slightly. However, the addition of Ni exceeding the Ni/Ru molar ratio of 1 : 1 resulted in a decrease in the yield of glycols and BDO compared with $RuNi_1$/AC. Based on the results of H_2-TPR with the Ru–Ni bimetallic catalysts (Fig. 2), the metal reduction peak in $RuNi_1$/AC shifted to the highest temperature among all the catalysts suggesting a strong interaction between Ru and Ni species. The interaction is expected to influence the yield of and selectivity to glycols during the hydrogenolysis of alginic acid. In addition, physically mixed Ru/AC + Ni/AC was prepared for investigating the effect of the Ru–Ni interaction on the

Table 3 Product yields and conversions obtained during the hydrogenolysis of reaction intermediates over Ru/AC in the NaOH solution[a]

Entry	Reactant	Liquid-product yield (%)								Conv. (%)
		EG	PDO	BDO	TOL	POL	LA	GA	FA	
1	Sorbitol	17.2	15.7	1.0	0.5	0.18	41.3	0	10.3	100
2	Mannitol	14.8	15.6	1.2	0.4	0	45.1	0	10.0	100
3	Xylitol	15.4	12.8	1.4	1.0	0	41.6	0	10.0	100
4	Lactic acid	0	1.7	0	0	0	98.3	0	0	1.7
5	Glycolic acid	4.6	0	0	0	0	0	95.4	0	4.6

[a] EG = ethylene glycol, PDO = 1,2-propanediol, BDO = 1,2-butanediol, TOL = tetritols (erythritol and threitol), POL = pentitols (xylitol, arabitol, and adonitol), LA = lactic acid, GA = glycolic acid, FA = formic acid; reaction conditions: at 210 °C for 2 h under 50 bar in 100 mM basic solution.

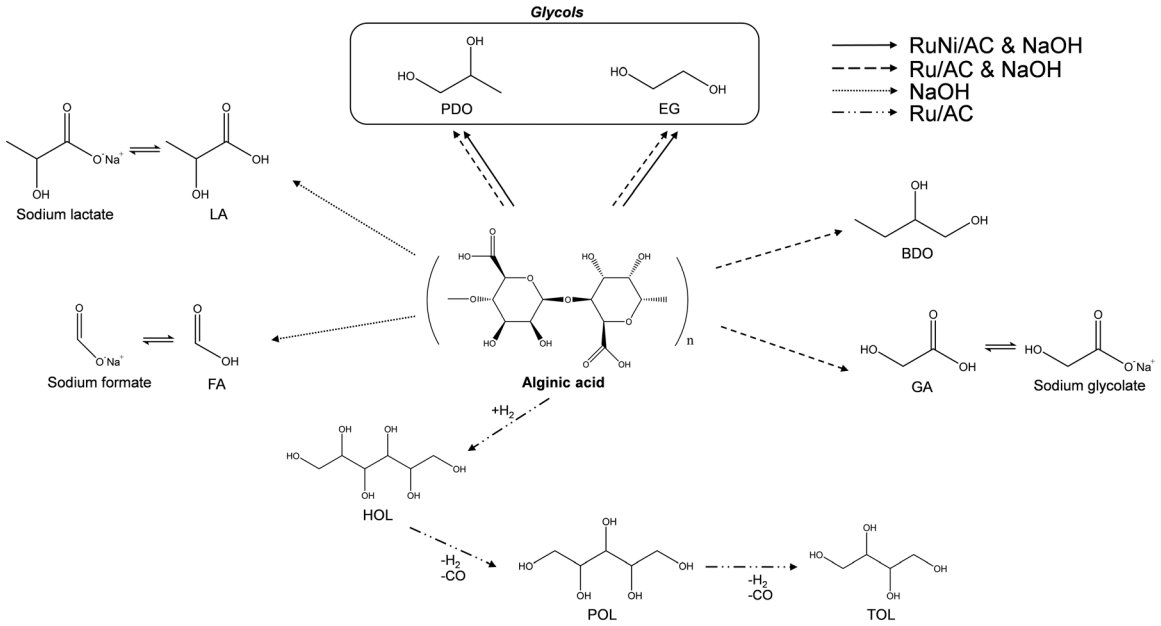

Scheme 1 Pathway for the catalytic hydrogenolysis of alginic acid depending on the catalytic conditions. Product notation: EG = ethylene glycol, PDO = 1,2-propanediol, BDO = 1,2-butanediol, TOL = tetritols (erythritol and threitol), POL = pentitols (xylitol, arabitol, and adonitol), HOL = hexitols (sorbitol, mannitol, and galactitol) LA = lactic acid, GA = glycolic acid, FA = formic acid.

reactivity. Ru/AC used for physical mixing contains about 8.8 wt% Ru as evidenced by ICP-AES, which is well-dispersed on the activated carbon based on the HAADF-STEM image (not shown). Ru/AC and Ni/AC were mixed physically at a 1 : 1 ratio, which is similar to the amount of Ru and Ni loaded in $RuNi_1$/AC. Reaction results as shown in Fig. 4 clearly indicate that the physically mixed Ru/AC + Ni/AC sample did not promote the yield of and selectivity to glycols compared to $RuNi_1$/AC, suggesting that the bimetallic structure of Ru and Ni is truly effective. Hence, the bimetallic Ru–Ni species, which was formed well when at a Ni/Ru molar ratio of 1 : 1, most actively promoted the conversion of alginic acid to glycols *via* hydrogenolysis.

Based on the reaction results, the pathway of alginic acid hydrogenolysis depending on the catalytic conditions can be proposed as shown in Scheme 1. Ru/AC in a neutral solution undergoes hydrogenation of alginic acid to HOL, followed by conversion to POL and TOL *via* decarbonylation. However, further decarbonylation of TOL rarely occurred resulting in the lack of production of shorter polyols such as EG, PDO, and BDO. In the presence of NaOH solution without Ru/AC, alginic acid is converted to organic acids, mainly LA and FA. However, alginic acid decomposes into various organic acids including GA and short-chain polyols such as glycols and BDO over Ru/AC in the presence of NaOH solution. Such organic acids from alginic acid may exist in the form of sodium salts inhibiting the conversion to glycols. The use of a basic solution alters the reaction pathway from decarbonylation to retro-aldol reaction. Glycols, the target products, are produced directly *via* internal C–C bond cleavage, suggesting that sugar alcohols or organic acids do not act as intermediates during the hydrogenolysis of alginic acid to glycols. Furthermore, bimetallic Ru–Ni supported on activated carbon promotes the hydrogenolysis of alginic acid resulting in increased yield of and selectivity to glycols and carbon efficiency.

4. Conclusions

Alginic acid was successfully converted to glycols such as ethylene glycol and 1,2-propanediol *via* hydrogenolysis over Ru-based activated carbon in a basic solution. In addition, various organic acids such as lactic acid, glycolic acid, and formic acid in the form of salts were produced. The type and concentration of the basic promoter strongly influenced the product distribution. Based on the hydrogenolysis of potential intermediates that can be produced from alginic acid under similar conditions, the direct conversion of alginic acid to glycols occurs *via* a retro-aldol reaction without intermediates such as sugar alcohols or organic acids under hydrogenolysis reaction conditions. The addition of Ni to activated carbon-supported Ru catalysts improved the yield of and selectivity to glycols obtained from alginic acid, and the optimal Ni/Ru molar ratio was 1 : 1. Furthermore, the positive effect of bimetallic RuNi catalysts was verified by comparison with physically mixed Ru and Ni supported on activated carbon. The highest yield of glycols was 24.1% when $RuNi_1$/AC was used in the presence of 100 mM NaOH. It is suggested that Ru–Ni bimetallic species formed *via* strong interaction between Ru and Ni result in the enhanced hydrogenolysis of alginic acid to glycols.

Conflicts of interest

There are no conflicts to declare.

Acknowledgements

This research was supported by a grant (2018R1A2B200516813) awarded by the Basic Science Research Program through the National Research Foundation of Korea (NRF) funded by the Ministry of Education. The Institute of Engineering Research at Seoul National University partially provided research facilities for this work.

Notes and references

1 V. Menon and M. Rao, *Prog. Energy Combust. Sci.*, 2012, **38**, 522–550.
2 G. Morales, J. A. Melero, J. Iglesias, M. Paniagua and C. López-Aguado, *React. Chem. Eng.*, 2019, **4**, 1834–1843.
3 A. J. Ragauskas, G. T. Beckham, M. J. Biddy, R. Chandra, F. Chen, M. F. Davis, B. H. Davison, R. A. Dixon, P. Gilna and M. Keller, *Science*, 2014, **344**, 1246843.
4 K. W. Chew, J. Y. Yap, P. L. Show, N. H. Suan, J. C. Juan, T. C. Ling, D.-J. Lee and J.-S. Chang, *Bioresour. Technol.*, 2017, **229**, 53–62.
5 K. A. Jung, S.-R. Lim, Y. Kim and J. M. Park, *Bioresour. Technol.*, 2013, **135**, 182–190.
6 C. Ban, W. Jeon, H. C. Woo and D. H. Kim, *ChemSusChem*, 2017, **10**, 4891–4898.
7 C. Ban, S. Yang, H. Kim and D. H. Kim, *Appl. Catal., A*, 2019, **578**, 98–104.
8 C. Ban, S. Yang, H. Kim and D. H. Kim, *Catal. Today*, 2020, **352**, 66–72.
9 I. M. Leo, M. L. Granados, J. Fierro and R. Mariscal, *Appl. Catal., B*, 2016, **185**, 141–149.
10 J. Sun and H. Liu, *Green Chem.*, 2011, **13**, 135–142.
11 Y. Amada, Y. Shinmi, S. Koso, T. Kubota, Y. Nakagawa and K. Tomishige, *Appl. Catal., B*, 2011, **105**, 117–127.
12 D. Götz, M. Lucas and P. Claus, *React. Chem. Eng.*, 2016, **1**, 161–164.
13 N. Ji, T. Zhang, M. Zheng, A. Wang, H. Wang, X. Wang and J. G. Chen, *Angew. Chem., Int. Ed.*, 2008, **47**, 8510–8513.
14 P. Lazaridis, S. Karakoulia, C. Teodorescu, N. Apostol, D. Macovei, A. Panteli, A. Delimitis, S. Coman, V. Parvulescu and K. Triantafyllidis, *Appl. Catal., B*, 2017, **214**, 1–14.
15 M. Liu, H. Wang, J. Han and Y. Niu, *Carbohydr. Polym.*, 2012, **89**, 607–612.
16 E. P. Maris and R. J. Davis, *J. Catal.*, 2007, **249**, 328–337.
17 S. Mondal, H. Malviya and P. Biswas, *React. Chem. Eng.*, 2019, **4**, 595–609.
18 C. Montassier, J. Menezo, L. Hoang, C. Renaud and J. Barbier, *J. Mol. Catal.*, 1991, **70**, 99–110.
19 Y. Nakagawa and K. Tomishige, *Catal. Surv. Asia*, 2011, **15**, 111–116.
20 D. Sohounloue, C. Montassier and J. Barbier, *React. Kinet. Catal. Lett.*, 1983, **22**, 391–397.
21 K. Wang, M. C. Hawley and T. D. Furney, *Ind. Eng. Chem. Res.*, 1995, **34**, 3766–3770.
22 X. Jin, B. Subramaniam and R. V. Chaudhari, in *Novel Materials for Catalysis and Fuels Processing*, ACS Publications, 2013, pp. 273–285.
23 D. G. Lahr and B. H. Shanks, *Ind. Eng. Chem. Res.*, 2003, **42**, 5467–5472.
24 A. Marinoiu, C. Cobzaru, E. Carcadea, C. Capris, V. Tanislav and M. Raceanu, *React. Kinet., Mech. Catal.*, 2013, **110**, 63–73.
25 M. Rivière, N. Perret, A. Cabiac, D. Delcroix, C. Pinel and M. Besson, *ChemCatChem*, 2017, **9**, 2145–2159.
26 J. Zhou, M. Zhang, L. Zhao, P. Li, X. Zhou and W. Yuan, *Catal. Today*, 2009, **147**, S225–S229.
27 M. Banu, P. Venuvanalingam, R. Shanmugam, B. Viswanathan and S. Sivasanker, *Top. Catal.*, 2012, **55**, 897–907.
28 X. Chen, X. Wang, S. Yao and X. Mu, *Catal. Commun.*, 2013, **39**, 86–89.
29 A. Perosa and P. Tundo, *Ind. Eng. Chem. Res.*, 2005, **44**, 8535–8537.
30 A. G. Sergeev and J. F. Hartwig, *Science*, 2011, **332**, 439–443.
31 J. H. Sinfelt, J. Carter and D. Yates, *J. Catal.*, 1972, **24**, 283–296.
32 L. S. Ribeiro, J. J. Delgado, J. J. Órfão and M. F. R. Pereira, *Appl. Catal., B*, 2017, **217**, 265–274.
33 L. Yang, J. Su, S. Carl, J. G. Lynam, X. Yang and H. Lin, *Appl. Catal., B*, 2015, **162**, 149–157.
34 T. Komanoya, H. Kobayashi, K. Hara, W.-J. Chun and A. Fukuoka, *Appl. Catal., A*, 2011, **407**, 188–194.
35 A. Calafat, J. Laine, A. López-Agudo and J. Palacios, *J. Catal.*, 1996, **162**, 20–30.
36 C. Crisafulli, S. Scire, R. Maggiore, S. Minico and S. Galvagno, *Catal. Lett.*, 1999, **59**, 21–26.
37 M. Cerro-Alarcón, A. Guerrero-Ruíz and I. Rodrıguez-Ramos, *Catal. Today*, 2004, **93**, 395–403.
38 W. Jeon, C. Ban, G. Park, T.-K. Yu, J.-Y. Suh, H. C. Woo and D. H. Kim, *J. Mol. Catal. A: Chem.*, 2015, **399**, 106–113.
39 F. Jin, J. Yun, G. Li, A. Kishita, K. Tohji and H. Enomoto, *Green Chem.*, 2008, **10**, 612–615.
40 D. Esposito and M. Antonietti, *ChemSusChem*, 2013, **6**, 989–992.
41 P. J. Hausoul, L. Negahdar, K. Schute and R. Palkovits, *ChemSusChem*, 2015, **8**, 3323–3330.
42 K. Niemelä and E. Sjöström, *Carbohydr. Res.*, 1985, **144**, 93–99.
43 K. Niemelä and E. Sjöström, *Carbohydr. Res.*, 1985, **144**, 241–249.